

Radiation transport modelling in divertors with the EIRENE code

D. Reiter¹, S. Wiesen¹, M. Born²

¹*Institut für Plasmaphysik, Forschungszentrum Jülich GmbH, EURATOM Association, Trilateral Euregio Cluster, D-52425 Jülich, Germany*

²*Philips Research Laboratories, Weisshausstrasse 2, D-52066 Aachen, Germany*

Abstract

Opacity effects, in particular of Lyman lines, in divertors are believed to be relevant for plasma spectroscopy and for the overall divertor dynamics through possible redistribution of excited hydrogen atoms and radiation losses. Quite elaborate computational radiation transport tools have been developed, specialized for numerous applications. The task in fusion research has been adaptation to fusion edge plasma conditions. In this paper we start from an existing kinetic neutral particle code already well adapted to divertor applications, and extend this from the “particle” simulation to an analogue “photon gas” simulation. It is shown how this can be achieved and that a quite flexible and detailed divertor radiation transport code can conveniently be obtained. We apply this to study Lyman opacity effects on population kinetics and hydrogen divertor radiation losses.

1 Introduction

Opacity effects, in particular on the resonance Lyman lines, have already been observed experimentally and computationally for dense divertor plasma conditions in various Tokamaks, e.g. Alcator C-MOD and they may be quite relevant for ITER-FEAT [1]. For example volume recombination, a crucial effect in detached divertor states, is expected to be reduced significantly by resonant photon re-absorption. Previous computational assessments are usually based upon highly idealized, often zero dimensional approximations (so called optical escape factors in collisional radiative models) [2]. Due to the spatial gradients of neutral gas profiles in divertors, the various line broadening mechanisms and the often kinetic (non-fluid) properties of the neutral gas components in divertors a quantitative bookkeeping of radiation processes seems to require Monte Carlo photon gas simulations also for dense divertors. Such procedures are already well established in many fields, e.g. in astrophysics, or for low and high pressure discharges used e.g. for lighting purposes. The effort to adapt

these specialized codes to typical fusion edge plasma conditions is quite considerable, but some steps have already been undertaken, e.g. with the CRETIN code [1].

In this paper we take the opposite approach: in a joint effort with lighting industry the EIRENE neutral particle transport code [3], widely used in fusion edge plasma studies, is currently extended from its test particle (neutrals and ions) options towards photon gas simulations. The radiation transfer equation is mathematically analogue to the linear Boltzmann equation solved by EIRENE. Because of that most of the existing coding can be used directly for photon transport problems, with only minor modifications. This is outlined in the second and third section. The relevant line emission profiles (typically: Voigt profiles) have been implemented into EIRENE, the spatial distribution of emission can be treated by the routines already in place for volume recombination processes. Absorption coefficients can be formulated in the same format as the present atomic and molecular databases used by EIRENE, with the wavelength dependency replaced by an energy dependency.

In sections 4 and 5 we test the photon gas simulation by comparing our Monte Carlo solutions with semi-analytical results, such as population escape factors and in the thermodynamical limit (spectral line shapes vs. Planck'ian). The “conditional expectation estimator” technique, optional in EIRENE [3] since long, permits reduction of the Monte Carlo procedure to analytical solutions without any noise, for point sources and purely absorbing media. This allows to eliminate statistical noise even for highly opaque conditions, as long as scattering (other than stimulated emission) is neglected, which we will do in this paper. The EIRENE code has been fully parallelized for multi-processor machines, as routinely utilized in the 3D stellarator applications, [4]. We will, however, not use this option in this paper and all runs discussed below have been performed on an IBM RS/6000 workstation. In the final section we apply the extended code to a model typical of conditions expected in ITER-FEAT from B2-EIRENE simulations [5].

2 Basic linear transport equations for particles and photons

The material in this sections can be found in many textbooks, such as [6] on the Boltzmann equation, or [7] on radiation transport in stellar atmospheres. Here we only give a brief “dictionary” for translating the terminology typical of radiation transport into that of neutral particle- (or also neutron-) transport.

The basic quantity of interest in photon gas transport is, usually the specific intensity (also: “brightness”) $I_\nu = I_\nu(\vec{x}, \nu, \vec{\Omega}, t)$. It has the dimensions: energy (time)⁻¹ (area)⁻¹ (solid angle)⁻¹ (frequency)⁻¹.

We first convert the frequency ν into an energy E , $E = h\nu$ with Planck’s constant h . Then the velocity space coordinates of a single ray $(E, \vec{\Omega})$ can be transformed into the velocity vector \vec{v} , on which, usually, neutral particle transport codes for fusion edge plasmas are based. In order to recover the energy E , the frequency needs to be added to the phase space of a test particle in the case of photons, $E = h\nu$, whereas for neutral atoms or molecules the mass is needed: $E = m/2|v^2|$.

Now we can identify the specific intensity I with the “energy transport flux” $\tilde{I} = \tilde{I}(\vec{x}, \vec{v}, t)$,

$$\tilde{I} = E \cdot v \cdot f(\vec{x}, \vec{v}, t) \tag{1}$$

and f is the usual particle distribution function, and $v = c$, the speed of light. The Monte Carlo code EIRENE solves the linear Boltzmann equation for the transport flux $\Phi (= v \cdot f)$ and provides responses $\langle g, \Phi \rangle$ for arbitrary (problem specific) “detector functions” $g(\vec{x}, \vec{v}, t)$. The brackets are to be understood as phase space integrals of $g \cdot \Phi$

Choosing $g = E$, we see that kinetic neutral particle transport codes also solve the radiation transfer equation for I as a special case.

The photon flux F across a surface normal to the ray directly corresponds to the (scalar) transport flux Φ and is the first angular moment of the specific intensity I :

$$F = \int I \cos(\theta) d\Omega = \int I \cos(\theta) \sin(\theta) d\theta d\phi \tag{2}$$

All responses computed from the neutral particle simulation codes for current plasma edge simulations tools as, e.g. B2-EIRENE ([8]), such as ionisation rates, surface fluxes, plasma cooling rates or momentum exchange rates (neutral - plasma friction) can, without any modification of the coding now also be obtained for the photon gas. The complication of nonlinearity in some collision integrals, resulting from the mutual influence of the radiation field and the excited state population of neutral particles can be dealt with by the same iteration procedure as it is already available for neutral-neutral particle collisions ([9]).

The volumetric source function for neutral particles, for example due to plasma recombination, can be re-interpreted as the photon emissivity for the case of radiation

transfer. The external volumetric source for neutral atoms, for example, due to recombination of plasma electrons and ions, reads

$$S_{rec}(\vec{r}, \vec{v}) = n_e(\vec{r}) \cdot n_i(\vec{r}) \cdot \langle \sigma v_e \rangle_{rec}(T_e, n_e) \cdot f_i(\vec{v})$$

The first 3 factors are the recombination rate, with $\langle \dots \rangle_{rec}$ the multi-step recombination rate coefficient [10]. Here f_i is the normalized ion distribution function, which is also used as initial distribution of atoms after recombination. It is, usually, a drifting Maxwellian. The corresponding photon emission term j_ν is given below, but it is obvious that only the recombination rate has to be replaced by the (spontaneous) emission rate, and that the velocity distribution f_i is replaced by the normalized emission line shape function $\Phi(\nu)$, determined by the line broadening mechanisms taken into account.

Absorption and scattering are entirely analogous in the two cases of photon gas and neutral gas simulation. Redistribution due to scattering of photons in the volume is described by the so called “phase function”, in case of neutral particles this same quantity is usually referred to as “scattering kernel”. The extinction coefficient $\chi(\vec{r}, \nu, t)$ (also: “opacity”, or “total absorption coefficient”) in radiation transport is the inverse of the photon mean free path, and, hence, the same quantity as the “total macroscopic cross section” Σ_t (Dimension: $(\text{length})^{-1}$) in neutron and neutral gas transport terminology [3].

3 Einstein coefficients

To describe emission and absorption processes for one spectral line microscopically, we consider two distinct energy levels in an atom with energies E_1 and E_2 (we assume $E_1 < E_2$ and $E_2 - E_1 = h\nu_0$) and statistical weights g_1 and g_2 . Then three processes can be identified:

1. **spontaneous emission:** This is determined by the Einstein A-coefficients, i.e., by $A_{21} = \text{transition probability per unit time for spontaneous emission}$ (units sec^{-1}). These coefficients are “rates” in the transfer equation, or, if divided by the upper level density: “rate-coefficients”. The line profile (see next item: absorption) is determined by the broadening mechanisms taken into account. Random sampling of the frequency from the convolution integral, if more than one broadening effect is included, can be done simply by sampling independently from the individual line profiles and then adding the random

numbers, due to a corresponding general law for sampling from convoluted distributions. Currently we have implemented Lorentz- and Doppler profiles, hence also Voigt profiles.

2. **absorption:** Due to the uncertainty principle for the energy levels (natural broadening) and other broadening processes like Doppler shift, the difference between the energy levels are not sharp. Photons with frequencies in the vicinity of the line center at ν_0 can be absorbed. The profile function $\Phi(\nu)$ is peaked at the line center and is normalized by

$$\int_0^\infty \Phi(\nu) d\nu = 1 \quad (3)$$

The *probability for absorption per unit time* is then $B_{12}\bar{J}$, where

$$\bar{J} = \int_0^\infty J_\nu \Phi(\nu) d\nu \quad (4)$$

is the frequency *integrated mean intensity* and where

$$J_\nu = \frac{1}{4\pi} \int I_\nu d\Omega \quad (5)$$

is the zeroth angular moment of I_ν . B_{12} is the so called Einstein B-coefficient for absorption.

3. **stimulated emission:** This is the only “true” scattering process included in the simulations below. It’s rate-coefficient is related to the B_{21} Einstein coefficient. This scattering is “coherent” (does not alter the frequency), nor the direction of a test-photon. In neutron transport such collision terms are referred to as delta-scattering or pseudo-collisions. Since the number of test-particles is altered, this corresponds, in this regard, to fission (neutrons) or, e.g., dissociation (neutral particles). Such processes are particularly trivial to include in Monte Carlo simulations as they only alter the weight of a test-flight along the trajectory. In radiation transport the corresponding scattering rates are usually absorbed in the absorption-rate.

Details about these three processes, in particular the Einstein relations between them, can be found in many textbooks. For the particular format needed to implement these as special case into existing neutral particle transport models we refer to the EIRENE web-domain [3].

4 Population escape factors

As a first check for the validity of the photon-transport simulations with EIRENE, we compare our Monte Carlo results with semi-analytical so called “population escape factors”. There are several different definitions of these factors in the literature. The one used here (and in the semi-analytical evaluation of Behringer, [2]) is given in [11]. We consider the population escape factor Θ_p from [2], defined as: holds:

$$\Theta_p = 1 - \frac{\int_{\Omega} \int_{line} \chi_{\nu}(x) I_{\nu}(x, \Omega) d\nu d\Omega}{4\pi j_{\nu}(x)} = 1 - \frac{G}{E} \quad (6)$$

where $\chi_{\nu}(x)$ is a spatially varying absorption coefficient for photons, $j_{\nu}(x)$ the emission coefficient, I_{ν} the spectral intensity and $d\Omega$ the solid angle element. Note that the emission and absorption profile is included in χ_{ν} and j_{ν} respectively. The numerator is the number of absorption processes in the plasma G at position x and the denominator is the number of emission processes E (both per unit volume and time).

This correction factor for Einstein coefficients in collisional radiative models is a function of the “optical thickness” τ , or, if the profile function $\Phi(\nu)$ is given, of $\tau_0 = \chi(\nu_0)b$. b is the characteristic length in the plasma and $\chi(\nu_0)$ is the absorption coefficient in the line center. $\Theta_p(x)$ furthermore depends upon the geometry. It is not a local quantity, since the source of photons is distributed in the entire volume. This definition has to be carefully distinguished from the “line escape factors”, which are more relevant for spectroscopic applications, but, due to a spatial delta distribution in the source, trivial for Monte Carlo evaluation.

In order to reproduce the semi-analytical population escape factors for Lyman α , Lyman β , Lyman γ and Lyman δ lines of hydrogen given in [2] we simulate a homogeneous hydrogen plasma in a cylinder of radius $b = 5 \text{ cm}$. The “plasma” consists of hydrogen in the ground-state $n = 1$ and upper excited states $n = 2, 3, ..$ for the Lyman lines. The parameters chosen here are $n_H = 10^{14} \text{ cm}^{-3}$ and $T_H = 1 \text{ eV}$. The density of the excited state atoms is irrelevant for these factors. Emission and absorption was modelled as described above, with Doppler broadening (again 1 eV) as the only line broadening mechanism. Fig. 1 compares the numerical results from [2] with our Monte Carlo calculations for the Lyman lines, both taken on the axis of the cylinder. The population escape factors Θ_p for Lyman β, γ, δ can perfectly be matched. The result for Lyman α has the largest statistical noise (0.2 % for the

absorption rate on axis) , due to high opacity (about 27) for this line, but also agrees perfectly within the statistical error bars.

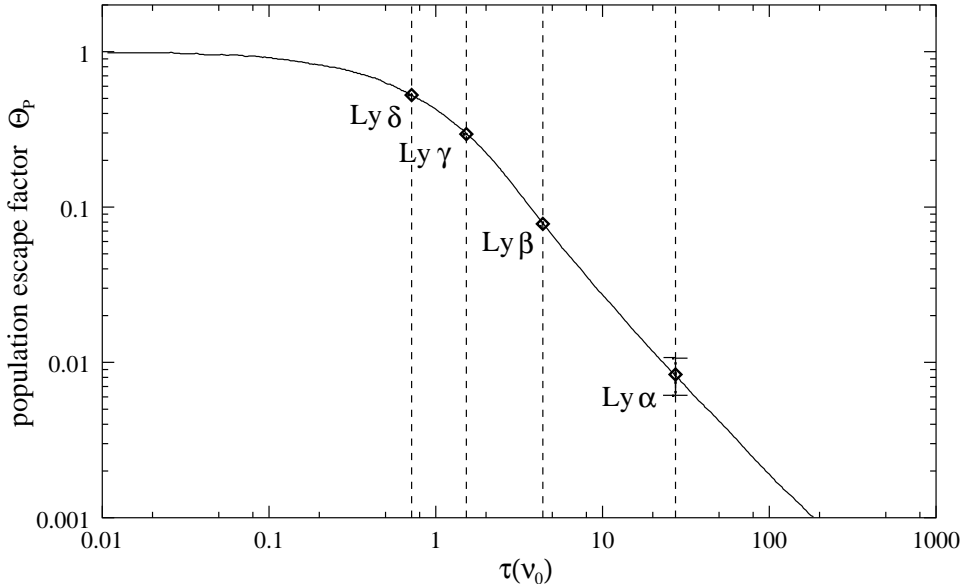


Figure 1: Population escape factors Θ_p for 4 different hydrogen Lyman lines. $\tau(\nu_0)$ is the optical depth in the line center. Solid line: [2], symbols: EIRENE simulation. Error bars are plotted for all lines, but are visible only in the highly opaque Lyman α case in this scale

5 Planck function for optically thick hydrogen Lyman α line

Because only the ratio of absorbed and emitted photon numbers enter into the population escape factor, the above validation does not check absolute values of the computed specific intensity function I_ν . This can be achieved by comparing the calculated spectral intensity with the Planck function for optically thick lines. In this optically thick limit the correctness of a kinetic Monte Carlo scheme requires particular attention. The Planck function,

$$B_\nu = \frac{2h\nu^3/c^2}{\exp\left(\frac{h\nu}{kT}\right) - 1} \quad (7)$$

represents the spectral intensity I_ν for the special case of blackbody radiation. We use the same geometry as in the previous section, except that now we treat a finite

cylinder (length: 10 cm). For the Hydrogen *Lyman* α line, which starts to become optically thick in our calculations at densities above 10^{14} cm^{-3} , the spectral intensity should approach the Planck curve from below, with increasing opacity, if the upper level density (emitting species) is kept in LTE with the lower. Fig. 5 shows Doppler broadened lines at different absorber densities in comparison to the Planck distribution. The temperature of the Hydrogen gas was again set to 1 eV, the densities of the upper $n = 2$ level is determined by Boltzmann distribution with this temperature.

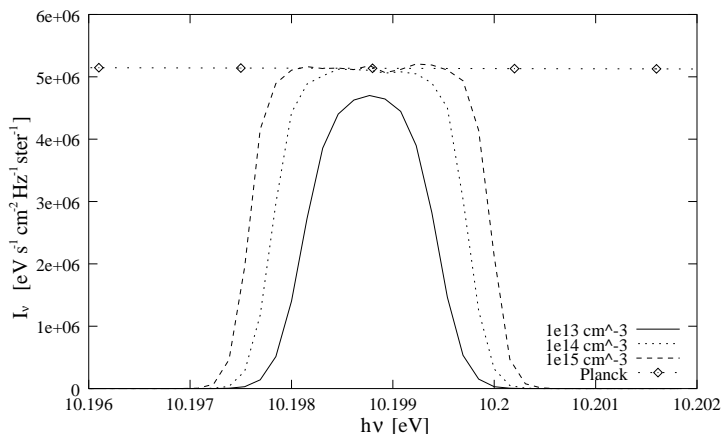


Figure 2: *Intensity functions of Lyman α radiation escaping from a cylinder 10 cm in diameter, 10 cm in length, in comparison to Planck's distribution. The intensity is plotted for 3 different absorber densities 1×10^{13} , 1×10^{14} and $1 \times 10^{15} \text{ cm}^{-3}$ at $kT = 1 \text{ eV}$. At higher densities the intensity is approximating the planck limit and flattens in the line center.*

The expected feature of approaching the Planck curve in the limit, in which even the photon gas is in thermodynamical equilibrium, is clearly recovered. This demonstrates that even a photon gas in thermal equilibrium is exactly modelled by our kinetic Monte Carlo approach, although, of course, it is patently foolish to use a Monte Carlo code under such conditions. The future goal still must be to optimise statistical performance near this limit, if a wide range from optically thin to optically thick has to be modelled in the same case.

6 Reformulated ionization and recombination rates

If we include photons of a certain line (say: of the Lyman α line) as explicit species in the kinetic neutral gas transport model, in addition to atoms and molecules, then the

effective ionization- and recombination rate coefficients used in the particle transport model also have to be revised, because these effective (density dependent) rate coefficients already include assumptions about radiation transport. The usual assumption is either “zero opacity”, then neglecting all re-absorption processes of photons in the balance equations for the excited state population coefficients, or perfect opacity. In this latter case the corresponding radiative transition rates (e.g., for Lyman lines: $A_{n,1}$) are set to zero. Intermediate is the concept of “population escape factors”, which are multiplicative factors to these rates $A_{i,k}$ obtained from semi-analytical evaluations of photon transport in idealized geometries (cylinders, spheres, etc.) and for simple profiles (usually: constant) of the emission and absorption profiles, see section 4 and [2].

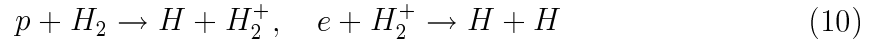
For our combined neutral atom - photon gas simulation we first have to eliminate the relevant transition rate (here: $A_{2,1}$) from the rate equations of excited state populations, because this rate now is explicitly included in the source term for the Lyman α photons. Doing so, the $n=2$ level of hydrogen atoms becomes “metastable” in the collision-radiative model and has to be included as further new species in the multi-species atom - photon gas simulation. As already described in detail in [10], the usual collisional radiative ionization-recombination balance:

$$\frac{D}{Dt}n_1 = -s n_1 + \alpha n_{ion} + o.c. \quad (8)$$

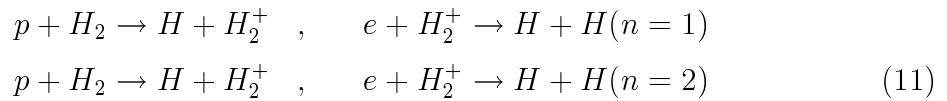
for ground state atom density n_1 now becomes

$$\begin{aligned} \frac{D}{Dt}n_1 &= -s_1 n_1 - s_{1,2} n_1 + s_{2,1} n_2 + \alpha_1 n_{ion} + o.c. \\ \frac{D}{Dt}n_2 &= -s_2 n_2 - s_{2,1} n_2 + s_{1,2} n_1 + \alpha_2 n_{ion} + o.c. \end{aligned} \quad (9)$$

Here s and α are the effective rate coefficients (density and temperature dependent) which include the effects of the “lumped species”, (terminology from air pollution modelling), in our case of the higher excited atoms. D/Dt is the total (convective) derivative, and *o.c.* stands for “other collision terms”, such as contributions from dissociating molecules, recombining molecular ions (“MAR”) etc. For example, also the MAR rate coefficient:



now has to be replaced by two effective MAR rate coefficients:



The same applies for the other molecular channels leading to neutral atoms in the EIRENE model, i.e. dissociation into ground- and excited states, and for the destruction of negative ions. All these rate coefficients have been computed on the basis of the most recent extension of the collision-radiative code from K.Sawada and T.Fujimoto, [12] and are available on the EIRENE web domain [3].

7 Sample applications to ITER-FEAT conditions

The extended EIRENE code is employed here to study the effects of Lyman-opacity in divertors, with the particular conditions chosen here being taken from B2-EIRENE simulations of ITER-FEAT ([5]). Figures 3 and 4 display the plasma temperature and density, respectively, chosen in this sample application. A total power of 100 MW (50% in electrons and 50% in ions) was assumed to flow from the core into the edge region, with a plasma density of $4 \cdot 10^{19}$ there. Deuteron-, helium- and carbon ions had been included in the B2-EIRENE plasma flow simulation. The deuteron flow field is shown in figure 5.

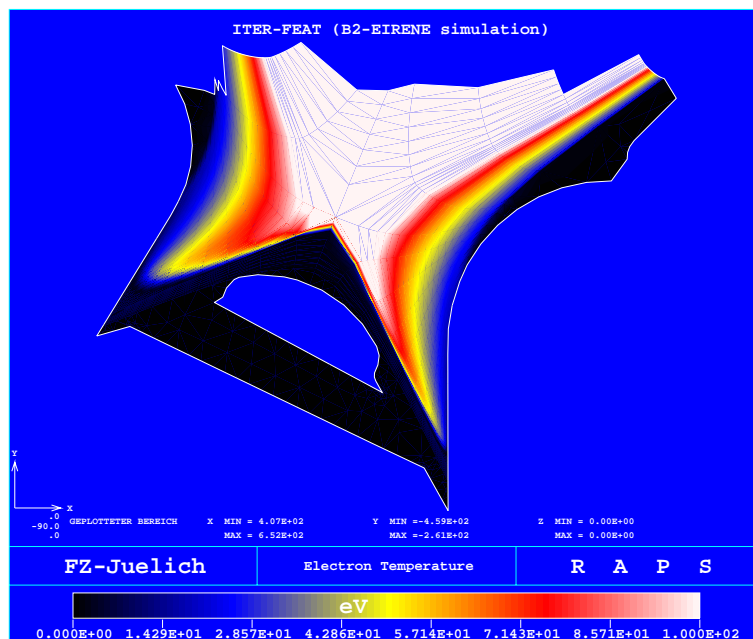


Figure 3: Electron temperature field (eV), from B2-EIRENE model.

Distinct from common B2-EIRENE simulations the 2d grid for the plasma field (as used in figure 5) has to be supplemented by a finite element discretisation of the

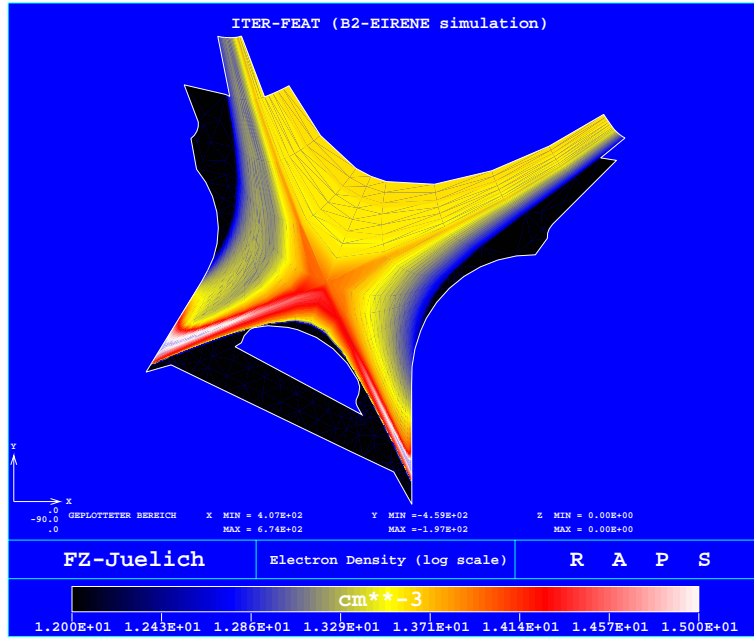


Figure 4: Electron density field (cm^{-3}), log.scale, from B2-EIRENE model.

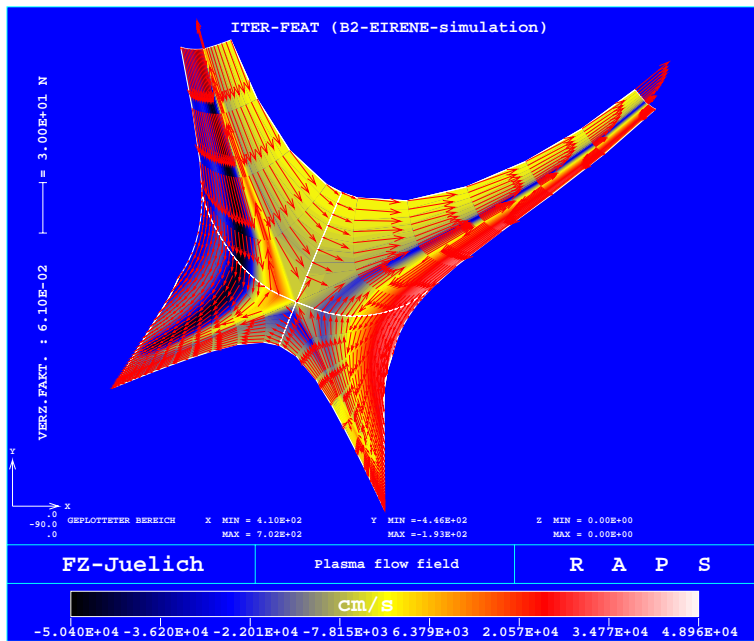


Figure 5: Deuteron ion flow field, from B2-EIRENE model. Blue colors in outer divertor and red colors in inner divertor indicate flow reversal

“vacuum region” between the outermost flux surface used in the plasma simulation and the vessel. This extension was already developed in [9] to allow for non-linear neutral-neutral interactions. This option permits spatial resolution of the neutral gas (and photon gas) field also in this domain. Neutral atom- and molecule density profiles are shown in figure 6 and 7. A small pump (recycling coefficient below one) was imposed at the bottom surface between the two divertor legs.

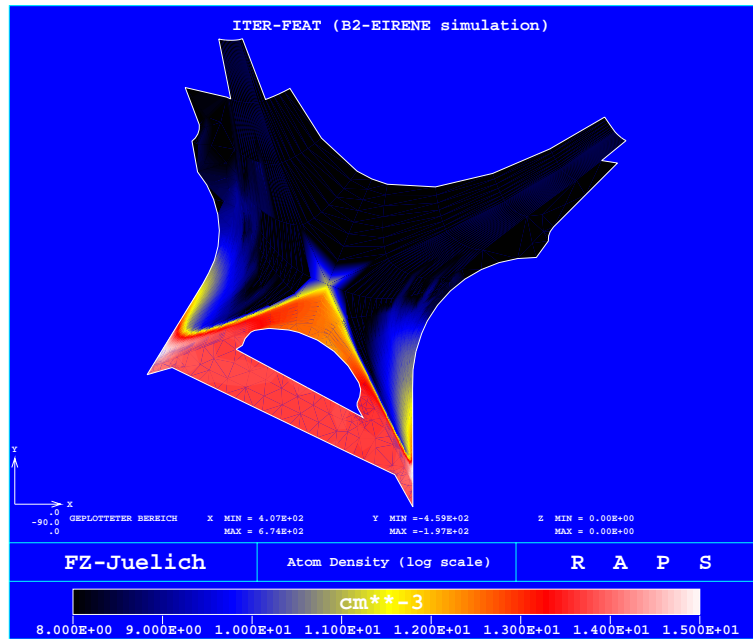


Figure 6: Neutral atom density, cm^{-3} , log. color scale, from B2-EIRENE model. Finite element spatial resolution outside the plasma domain included, for nonlinear Lyman α photon simulation.

From the ground state atom density profile and the plasma density and temperature we have derived the $n=2$ excited state density profile, on the basis of the ordinary (optically thin) collision-radiative population coefficients taken from the EIRENE database. This provides, for a first iteration step, the volumetric source of Lyman α photons. Doppler broadening is taken into account on the basis of the 2D temperature field of neutral atoms (the same for ground state and excited states in this first iteration.) The resulting photon gas density is shown in figure 8.

The total emissivity of this line was $8 \cdot 10^{24}$ photons per second. About 2/3 of this flux was re-absorbed in the volume, one third was absorbed at the vessel surfaces and the targets. About 5% of the total flux penetrates into the plasma core region

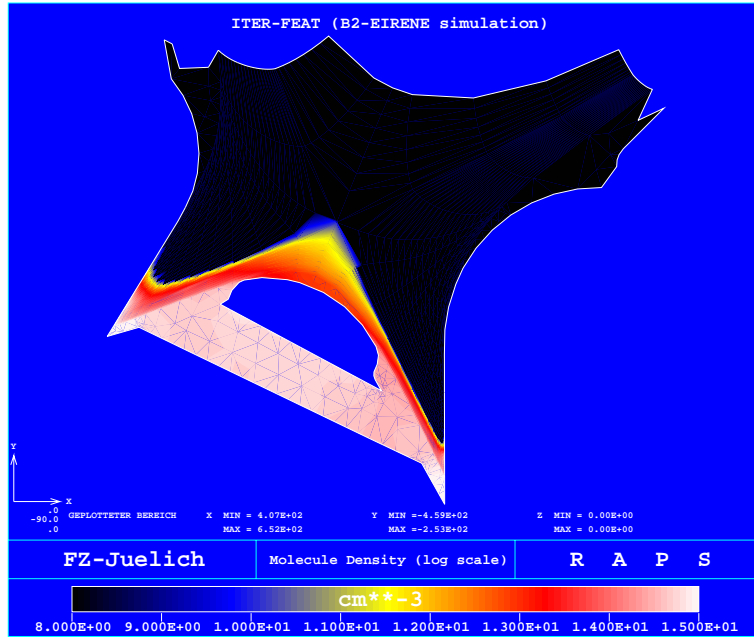


Figure 7: same as figure 6, but D₂ molecule density

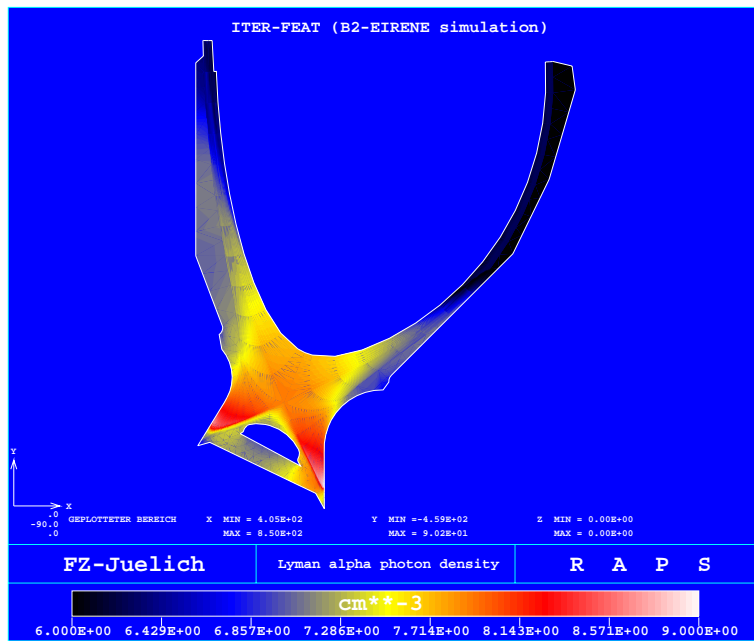


Figure 8: same as figure 6, but Lyman α photon density

not modelled here, only 5 % and 10 % are re-absorbed at the inner and outer target, respectively. Clearly, this first iteration will lead to a modification of the population

distribution, and hence, of the ionisation-recombination balance in the divertor and the hydrogen radiation losses to walls. The neutral atom densities of ground- and $n=2$ state as well as the photon density have to be iterated further, together with the plasma state, in the usual B2-EIRENE iteration scheme [8]. This and more details about the photon transport will be given in the final paper.

8 Conclusions and outlook

A fully parallelized 3D Monte Carlo neutral particle code for fusion edge plasma studies has been generalized to photon gas simulations (radiation transport). Doppler and Voigt broadened line emission profiles have been implemented, absorption in the volume as well diffuse and specular reflection at surfaces could be carried over from existing coding for neutral particles. The modified collision-radiative rate coefficients for transitions to and from the upper level of the Lyman α lines have been added to the atomic database for the EIRENE code. The code extensions have been validated against semi-analytical results (population escape factors) for idealized cases, up to quite high opacity (optical thickness of the order 30). Even transition to the optically dense blackbody radiation limit could be reproduced with high statistical precision. In first stand-alone applications the Lyman α line radiation transport has been included in an B2-EIRENE study of ITER-FEAT divertor conditions. Typically 2/3 of this radiation is found to be re-absorbed in the volume, 1/3 at the vessel. The non-linear response of absorption and emission on the neutral atom population and on the divertor hydrogen radiation, as well as on the ionization-recombination balance, still has to be investigated. Further extensions will also address Zeeman splitting.

References

- [1] Wan, A.S. et al., J.Nucl.Mat. Vol.220-222, p1102 (1995)
- [2] K. Behringer, "Escape factors for line emission and population calculations" MPI-Garching Report, IPP 10/11 (April 1998) and: Atomic Data Analysis Structure (ADAS), see "<http://adas.phys.strath.ac.uk>"
- [3] D.Reiter et al. see "<http://www.eirene.de>"
- [4] Feng, Y. et al., this conference
- [5] A.S.Kukushkin et al., in 18th Fusion Energy Conference, Oct.2000, IAEA-CN-77, paper ITERP/10(R), (2000)
- [6] Cercignani, C., "The Boltzmann Equation and Its Applications", Springer Verlag (1988)
- [7] Mihalas, D., "Stellar atmospheres", W.H.Freeman and Company, San Francisco, (1978)
- [8] Reiter, D., "Progress in 2-Dimensional Plasma Edge Modelling", J. Nucl. Mat., Vol.196-198, p241 (1992).
- [9] Reiter, D. et al., J.Nucl.Mat. Vol.220-222, p987 (1995)
- [10] Bates, D.R., Kingston,A.E., McWhirter, R.W.P., Proc. Roy. Soc. , Vol 270, p155 (1962)
- [11] Irons, F.E., J.Quant.Spectrosc. Radiat. Transf., Vol 22, p1 (1979)
- [12] W. Wuenderlich, U.Fantz, "A Collisional-Radiative Model for H2 and H: Extensions and Applications" MPI-Garching Report, IPP 10/17 (June 2001)